

square root of a complex signal, as follows:

$$RMS_{complex} = \left(\frac{\sum |z|^2}{N} \right)^{1/2} \quad (1)$$

$$|z|^2 = \left((I^2 + Q^2)^{1/2} \right)^2 \quad (2)$$

$$RMS_{complex} = \left(\frac{\sum (I^2 + Q^2)}{N} \right)^{1/2} \quad (3)$$

2. Methodology

The most basic of measurements of the radio signals from a given direction in the sky is the “total power”, or power response, which is obtained with the aid of a radio-detector system. There are several methods of observing modes for total power measurement and depend on the use or not of a temperature system reference (i.e. a noise diode). In the present study, there was no access to any temperature reference of the system, for this, a switching position observing method was used. The telescope moves between an offset position (OFF) (in relative or absolute coordinates) and a source position (ON). Optimally, the OFF position has a fixed azimuth and the same elevation than the target position to ensure that the ON and OFF positions are measured through the same air-mass. Relative position switching to a specific OFF position is required when observing complex emission regions (making it difficult to find an emission-free reference position) (Mangum et al., 2000). Using this procedure, the radio telescope moves between the ON and OFF sky positions in the OFF-ON-OFF-ON or OFF-ON-ON-OFF pattern. A sequence is composed of one or more repetitions of this basic cycle. This order of samples eliminates the effects on linear change measurements in atmospheric noise or receiver gain. It is possible to specify the integration time per position.

In order to perform a survey tests, calibration radio sources with well known fluxes to evaluate the switching position method to get total flux with the DS3 and without temperature reference were considered.

3. Calibrating Radio Sources

- **PKS 1934-638:** The first radio source chosen was PKS 1934-638, a Seyfert II galaxy. A high-resolution angular observations of PKS 1934-638 were made periodically over more than 20 years (Preston et al., 1989; Tzioumis et al., 1996; King, 1994) over a wide range of frequencies. More recently, Ojha et al. (2004) presented VLBI observations at 8.4 GHz PKS 1934-638 as part of a combined analysis of 30 years of observations.
- **PKS 0521-365:** The second source chosen was PKS 0521-365, a BL Lac. object (Falomo et al., 2009; Leon et al., 2016). Tingay et al. (1996) observed PKS 0521-365 in three times at 4.8 GHz and 8.4 GHz.

Both sources have been observed for more than two decades at different wavelengths or frequencies (see table 1). Their integrated flux along radio spectra are well

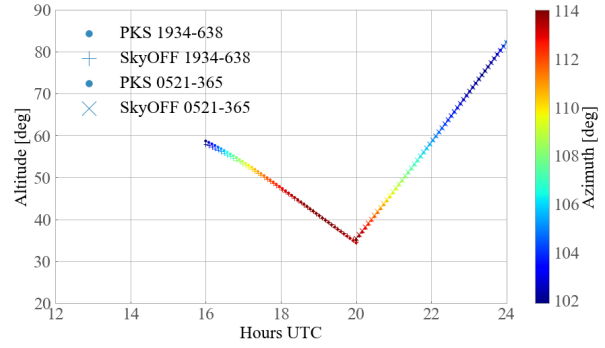


Figure 2: Observation plan.

known, and their flux distributions have been mapped on some frequencies. Both sources are being used as flux density calibrators for the Australia Telescope Compact Array (ATCA) at centimeter wavelengths, particularly PKS 1934-638 as primary calibrator and 0521-365 as secondary calibrator. Moreover, there are mathematical models that fit the observed data for each one of these sources.

The mathematical models published for each calibrator source, are:

For PKS 1934-638:

Model 1: 0 to 11 GHz. (Reynolds, 1994)

$$\log_{10}(S_\nu) = -30.7667 + 26.4908 \times \log_{10}(\nu) - 7.0977 \times \log_{10}(\nu)^2 + 0.605334 \times \log_{10}(\nu)^3$$

Model 2: 10 to 24 GHz. (Sault, 2003)

$$\log_{10}(S_\nu) = -202.6259 + 149.7321 \times \log_{10}(\nu) - 36.4943 \times \log_{10}(\nu)^2 + 2.9372 \times \log_{10}(\nu)^3$$

For PKS 0521-365, the model that fits the published data (SIMBAD database) for 80 to 8400 MHz, was obtained as part of the present work:

Model 3: 80 to 8400 MHz.

$$\log_{10}(S_\nu) = -869.78 + 822.42 \times \log_{10}(\nu)^{0.5} + 708.05 \times \log_{10}(\nu)^{-1} - 328.08 \times \log_{10}(\nu)^{0.75} - 374.06 \times \log_{10}(\nu)^{-2}$$

4. Results

Using the calibrating radio sources catalogue, Tab. 2, a survey test on DOY 038 2017 was performed. Fig. 2 shows the transit during the observation windows time for each source and the corresponding sky OFF position.

The signal contribution of the calibrating radio source (ON) by relative difference with the background (OFF), using the power calculated for each position ON/OFF as it was explained in Sec. 1.1., was calculated as,

$$Flux = \frac{(ON - OFF)}{OFF} \quad (4)$$

As is shown in Fig. 3a the data recorded by the DS3 for PKS 1934-638 using the switching position method allows to get a total flux approximation that fits with the published data and models. In Fig. 3b it can be seen the difference between the IFMS, each group of 4 channels has a gain offset that correspond with the internal calibration of the telecommunication system.

Table 1: Radio sources data fro SIMBAD database (Wenger et al., 2000)

RAJ2000 “h:m:s”	DEJ2000 “d:m:s”	Bname	Ident	Mag	z	S80 Jy	S408 Jy	S1410 Jy	S2700 Jy	S5000 Jy	S8400 Jy
05:22:58.010	-36:27:31.90	B0521-365	N	16.8	55	89	36.1	16.3	12.5	9.23	6.4
19:39:25.010	-63:42:45.70	B1934-638	G	18.4	185		6.24	16.4	11.5	6.13	3

Table 2: Catalogue information for the survey test

Name	RA	DEC
0521-365	05:22:57.984651	-36:27:30.850920
C0521OFF	05:22:57.984651	-37:27:30.850920
1934-638	19:39:25.026000	-63:42:45.630000
C1934OFF	19:39:25.026000	-64:42:45.630000

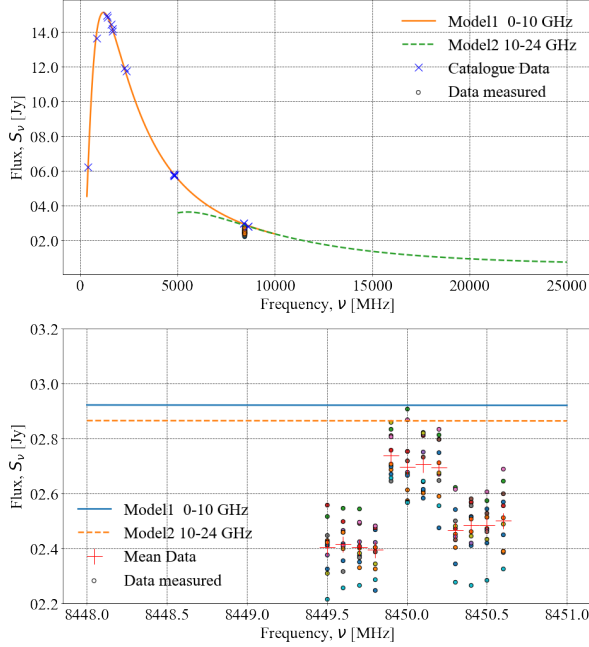


Figure 3: Upper panel: Shows the published PKS 1934-638 models for different frequency ranges and the published data with crosses. The dot points represents the acquired data by DS3. Lower panel: It is a zoom over the bandwidth observed by DA3, the error between the models and the data is 15%, and the offset between frequency channels is due to calibration between the IFMS devices.

Figure 4a shows the data recorded by the DS3 for PKS 0521-365, with the same; the total flux approximation fits with the published data and the proposed model. Again, Fig. 4b shows the difference between the IFMS.

5. Conclusions

From this work it is possible to show that DS3 is capable, with some limitations and choosing correctly the observation technique, of being a single dish radio telescope using the telecommunication devices installed. In order to avoid the limitations, be more flexible, and precise, the development of a specific device capable of handling more subchannels and maybe a wider bandwidth, is recommended.

Acknowledgements: The authors want to thank ITeDA, CONAE and ESA for their active participation and permanent support to this job. The collaboration of DS3 staff in order to carry out the observations, is deeply appreciated. The help and advice by Paula Benaglia

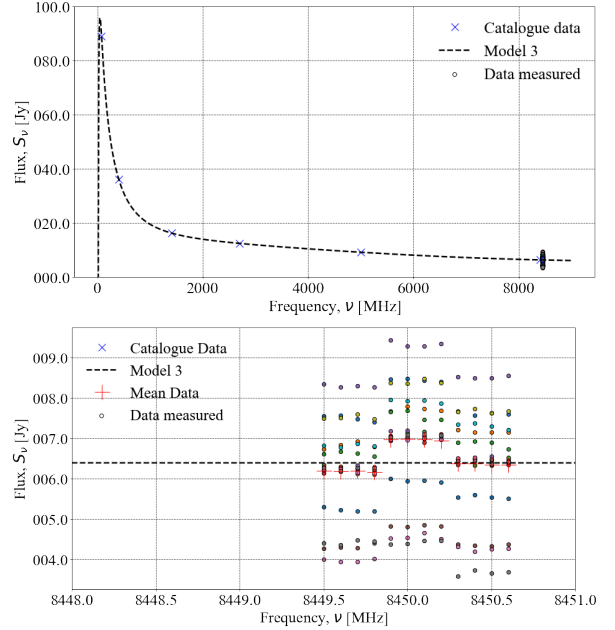


Figure 4: Upper panel: Shows the PKS 0521-365 proposed model and the published data with crosses. The dot points represents the acquired data by DS3. Lower panel: It is a zoom over the bandwidth observed by DS3, the error between the model and the data is less than 6%, and the offset between frequency channels is due to calibration between the IFMS devices.

in choosing the radio sources observed was fundamental for this reaseach. This publication will be included in the PhD thesis co-financed by CONICET "Procesamiento de Señales de Radio mediante computación paralela con GPU: Implementación para la DSA 3". by A. Cancio.

References

- Benaglia P., et al., 2011, Boletin de la Asociacion Argentina de Astronomia, 54, 447
- Cancio A., et al., 2016, Boletin de la Asociacion Argentina de Astronomia, 59
- Falomo R., et al., 2009, A&A, 501, 907
- King E., , 1994, Ph.D. thesis, Univ. Tasmania
- Leon S., et al., 2016, A&A, 586, A70
- Madde R., et al., 2007, Proceedings of the IEEE, 95, 2215
- Mangum J. G., Emerson D. T., Greisen E., 2000, ASP Conference Series 217, p. 179
- Ojha R., et al., 2004, The Astrophysical Journal Supplement Series, 150, 187
- Preston R. A., et al., 1989, AJ, 98, 1
- Reynolds J. E., , 1994, A Revised Flux Scale for the AT Compact Array, AT Memo 39.3/040
- Sault R. J., , 2003, ATCA flux density scale at 12mm, AT Memo 39.3/124
- Tingay S. J., et al., 1996, AJ, 111, 718
- Tzioumis A., et al., 1996, in Ekers R. D., Fanti C., Padrielli L., eds., IAU Symposium Vol. 175, Extragalactic Radio Sources. p. 73
- Wenger M., et al., 2000, A&AS, 143, 9